

# MAcNLOPS for $ZZ$ Pair Production at the LHC

Yuxiao Che\* and Rikkert Frederix†

*Department of Physics, Lund University, Box 118, 221 00 Lund, Sweden*

## Abstract

We present an implementation of the MAcNLOPS matching prescription for  $pp \rightarrow ZZ$  production in a MADGRAPH5\_AMC@NLO+PYTHIA8 setup. Starting from a standard MC@NLO event sample, negative  $\mathbb{H}$  events are removed and compensated by a veto applied to the first shower emission of the  $\mathbb{S}$  events. The implementation is validated against MC@NLO for radiation-sensitive and inclusive diboson observables. Agreement is found up to a rather small power-suppressed contribution affecting the very low- $p_T$  region. The method removes all negative  $\mathbb{H}$  weights with negligible additional computational cost, while negative  $\mathbb{S}$  weights are left unchanged, showing that MAcNLOPS is a promising alternative to MC@NLO with a reduced fraction of negative weights.

## 1 Introduction

Precision predictions for LHC observables are based on event generators that combine fixed-order perturbative accuracy with fully exclusive final states. In this context, NLO+PS matching is a baseline requirement for phenomenological studies and experimental analyses. The matching procedure must preserve the NLO accuracy of inclusive observables, describe the first hard QCD emission reliably, and at the same time remain compatible with the logarithmic structure, recoil prescription and event structure of the parton shower. These requirements are not independent, and different matching schemes realise the compromise between fixed-order accuracy, shower control and event-generation efficiency in different ways.

A canonical formulation of this problem is provided by the MC@NLO method [1]. Its central idea is to subtract from the real-emission matrix element the approximation already generated by the shower, and to add the corresponding integrated contribution to the Born-like event sample. This gives NLO-accurate predictions while leaving the subsequent shower evolution to the parton-shower program. The price paid for this generality is the appearance of events with negative weights. Negative weights do not invalidate the calculation: they are a consequence of the local cancellation structure of the matched cross section. They are, however, undesirable in practice. They reduce the statistical power of event samples, increase the number of generated events needed for a given precision, and complicate the use of simulated samples in experimental analyses.

Several approaches have been proposed to address this problem. In the POWHEG method [2,3], the hardest emission is generated with a positive Sudakov formulation based on the real matrix element. This largely avoids the negative-weight problem and has been highly successful phenomenologically, but it also changes the division of labour between the

---

\*E-mail: [yu7648ch-s@student.lu.se](mailto:yu7648ch-s@student.lu.se)

†E-mail: [rikkert.frederix@fysik.lu.se](mailto:rikkert.frederix@fysik.lu.se)

NLO calculation and the parton shower: the first emission is generated by the matching framework rather than by the shower itself. This distinction can be relevant when one wants to preserve, as much as possible, the logarithmic structure and recoil strategy of a given shower. Other methods, such as KrkNLO [4], also aim at positive-weight event samples, but are less straightforward to apply as fully general matching prescriptions.

Within the MC@NLO framework itself, a detailed analysis of the origin of negative weights led to the MC@NLO- $\Delta$  prescription [5]. This method modifies the MC@NLO matching formula by introducing a Sudakov-like factor  $\Delta$  in the  $\mathbb{H}$  contribution, together with a compensating term in the  $\mathbb{S}$  contribution. The factor is constructed from shower no-emission probabilities and suppresses  $\mathbb{H}$  events in regions where the parton shower gives an efficient description of the radiation. This reduces the negative  $\mathbb{H}$ -event component while preserving the NLO expansion and the hard-emission behaviour of the matched result. Consequently, MC@NLO- $\Delta$  can significantly improve the event-generation efficiency, but it does not remove the negative-weight problem altogether.

The MAcNLOPS method [6] provides a different route. It can be viewed as a minimal modification of the MC@NLO construction in which the regions where the shower approximation exceeds the real matrix element are treated multiplicatively, while the remaining regions retain an additive structure. In this way, the negative  $\mathbb{H}$ -event contribution of MC@NLO is removed and compensated by a veto procedure applied after the first shower emission. The method therefore keeps a key practical advantage of MC@NLO, namely that the first emission is still generated by the shower, while addressing one of its main efficiency limitations. In the implementation studied here, the focus is on this minimal MAcNLOPS mechanism and, in particular, on the removal of negative  $\mathbb{H}$  weights. Possible negative  $\mathbb{S}$  weights are a separate issue and are not eliminated by the procedure considered in this work.

More recently, the ESME framework, “Exponentiated Subtraction for Matching Events”, was introduced [7]. Like MAcNLOPS, it aims at positive-weight NLO+PS matching while retaining a close connection to the parton shower, but it addresses the problem more broadly by exponentiating the subtraction contribution associated with the NLO normalisation and treating it through an event-by-event accept–reject procedure. In this sense, ESME is conceptually more comprehensive than the minimal MAcNLOPS construction studied here.

The aim of this paper is to present a first implementation of this MAcNLOPS prescription for  $pp \rightarrow ZZ$  production, using MADGRAPH5\_AMC@NLO (MG5\_AMC) [8] interfaced to PYTHIA8 [9], and to validate it against standard MC@NLO. The  $pp \rightarrow ZZ$  process is a useful first application. Its Born-level final state is colour singlet, which avoids the additional complications associated with final-state QCD radiation from coloured particles, while being less trivial than a  $2 \rightarrow 1$  colour-singlet process. It therefore offers a controlled but meaningful environment in which to study the practical behaviour of MAcNLOPS. We compare the two approaches for radiation-sensitive and inclusive observables, both after the first shower emission and after the subsequent shower evolution. Particular attention is paid to the low-emission region, where the compensation of removed negative  $\mathbb{H}$  events is most delicate.

This paper is organised as follows. In Sects. 2 and 3, we review the formulation of MAcNLOPS and describe the implementation strategy used in this work. We present numerical results and compare them to standard MC@NLO in Sect. 4 and conclude in Sect. 5.

## 2 MAcNLOPS

We first review the form of the MAcNLOPS matching formula and then describe how it is implemented in the present calculation. Throughout this section, the formulae are written for a single real-emission sector. Sums over flavours, FKS sectors and parton luminosities are suppressed in the notation, but are included in the implementation. We assume a factorisation of the real-emission phase space,

$$d\Phi = d\Phi_B d\Phi_R, \quad (1)$$

where  $\Phi_B$  denotes the underlying Born phase space and  $\Phi_R$  the radiation variables.

In MC@NLO matching [1], the hard-event generation can be written in terms of two event classes. The  $\mathbb{S}$  events have Born kinematics, while the  $\mathbb{H}$  events have real-emission kinematics, schematically,

$$\mathcal{F}^{(\mathbb{S})}(\Phi_B) = \mathcal{B}(\Phi_B) + \mathcal{V}(\Phi_B) + \int \mathcal{K}(\Phi_B, \Phi_R) d\Phi_R \equiv \tilde{\mathcal{B}}(\Phi_B), \quad (2)$$

$$\mathcal{F}^{(\mathbb{H})}(\Phi) = \mathcal{R}(\Phi) - \mathcal{K}(\Phi). \quad (3)$$

Here  $\mathcal{B}$ ,  $\mathcal{V}$  and  $\mathcal{R}$  denote the Born, virtual and real-emission contributions, respectively. The quantity  $\mathcal{K}$  is the Monte Carlo counterterm, i.e., the shower approximation to the real-emission matrix element in the corresponding singular region. It removes the part of the real-emission contribution that would otherwise be generated again by the parton shower.

The origin of negative  $\mathbb{H}$  weights is apparent from Eq. (3). Whenever the shower approximation locally exceeds the real matrix element,  $\mathcal{K}(\Phi) > \mathcal{R}(\Phi)$ , the  $\mathbb{H}$ -event weight is negative. This is not a pathology of the matched cross section, since the negative contribution is compensated by the showered  $\mathbb{S}$  events, but it is inefficient for event generation. The purpose of MAcNLOPS is to explicitly perform this cancellation between the  $\mathbb{H}$  and  $\mathbb{S}$  events at the level of the hard cross section,

$$\mathcal{F}^{(\mathbb{S}+\text{PS})}(\Phi) = \left( \tilde{\mathcal{B}}(\Phi_B) \otimes \text{PS}_1(\Phi) \right) \otimes \mathcal{P}_{\text{veto}}(\Phi) \quad (4)$$

$$\mathcal{F}_+^{(\mathbb{H})}(\Phi) = (\mathcal{R}(\Phi) - \mathcal{K}(\Phi)) \Theta(\mathcal{R} - \mathcal{K}), \quad (5)$$

by removing the negative contributions from the  $\mathbb{H}$  events, through the inclusion of the theta function in Eq. (5), and vetoing a corresponding fraction of the  $\mathbb{S}$  events. In Eq.(4), for a Born configuration  $\Phi_B$ , the first shower emission gives either no resolvable emission above the shower cut-off or a real-emission phase-space point  $\Phi$ . Schematically, the corresponding one-emission shower probability can be written as

$$\text{PS}_1(\Phi) = \Delta(t_{\text{cut}}, \Phi_B) + \frac{\mathcal{K}(\Phi)}{\mathcal{B}(\Phi_B)} \Delta(t, \Phi_B) d\Phi_R, \quad (6)$$

where  $\Delta(t, \Phi_B)$  is the shower Sudakov factor and  $t$  is the shower ordering variable. The first term corresponds to no emission above the cut-off  $t_{\text{cut}}$ , while the second term corresponds to a first emission at scale  $t$ . The MAcNLOPS modification in Eq.(4) consists of accepting the one-step showered  $\mathbb{S}$  events with the probability

$$\mathcal{P}_{\text{veto}}(\Phi) = 1 + \frac{\mathcal{R}(\Phi) - \mathcal{K}(\Phi)}{\mathcal{K}(\Phi)} \Theta(\mathcal{K}(\Phi) - \mathcal{R}(\Phi)), \quad (7)$$

and removing the events from the sample otherwise.

Thus, in the region of the real-emission phase space where the shower overestimates the real matrix element, the negative  $\mathbb{H}$  events are explicitly removed by a theta function, and, at the same time, a fraction of the  $\mathbb{S}$  events is deleted after the first shower emission, with a probability  $1 - \mathcal{P}_{\text{veto}}(\Phi)$ . In the complementary region, where the real matrix element is larger than the shower approximation and event weights are already positive, the usual additive  $\mathbb{H}$  contribution is retained. The resulting MACnLOPS cross section is therefore

$$\begin{aligned}
d\sigma_{\text{MACnLOPS}} &= \tilde{\mathcal{B}}(\Phi_B) \Delta(t_{\text{cut}}, \Phi_B) d\Phi_B \\
&+ \tilde{\mathcal{B}}(\Phi_B) \frac{\mathcal{K}(\Phi)}{\mathcal{B}(\Phi_B)} \Delta(t, \Phi_B) \left[ 1 + \frac{\mathcal{R}(\Phi) - \mathcal{K}(\Phi)}{\mathcal{K}(\Phi)} \Theta(\mathcal{K}(\Phi) - \mathcal{R}(\Phi)) \right] d\Phi \\
&+ [\mathcal{R}(\Phi) - \mathcal{K}(\Phi)] \Theta(\mathcal{R}(\Phi) - \mathcal{K}(\Phi)) d\Phi.
\end{aligned} \tag{8}$$

The last term is manifestly positive. For the second term, the factor in square brackets is between zero and one, and does not introduce (additional) negative  $\mathbb{S}$  weights. Therefore, negative  $\mathbb{H}$  weights are removed. Possible negative  $\mathbb{S}$  weights, originating from  $\tilde{\mathcal{B}}(\Phi_B) < 0$ , are not addressed by this procedure, but can be reduced through folding [5, 10–12] and/or Born spreading [13].

The NLO accuracy follows directly by comparing Eq. (8) with the standard MC@NLO expression. In the region  $\mathcal{R}(\Phi) > \mathcal{K}(\Phi)$ , the MACnLOPS expression is identical to MC@NLO. In the region  $\mathcal{K}(\Phi) > \mathcal{R}(\Phi)$ , their difference is proportional to

$$\left[ \frac{\tilde{\mathcal{B}}(\Phi_B)}{\mathcal{B}(\Phi_B)} \Delta(t, \Phi_B) - 1 \right] [\mathcal{R}(\Phi) - \mathcal{K}(\Phi)] \Theta(\mathcal{K}(\Phi) - \mathcal{R}(\Phi)). \tag{9}$$

The difference  $\mathcal{R} - \mathcal{K}$  is non-singular, since the two terms have the same soft and collinear limits. The factor in the first square bracket starts only beyond leading order. Hence the difference between MACnLOPS and MC@NLO is of NNLO size for infrared-safe observables. The two prescriptions therefore have the same NLO accuracy, while differing by matching-level higher-order terms.

### 3 Implementation and validation

The implementation follows directly from Eq. (8). Starting from a standard MC@NLO event sample generated with MG5\_AMC [8] in the default setup<sup>1</sup>, the negative  $\mathbb{H}$  events are removed from the final sample and their contribution is compensated by applying the veto probability in Eq. (7) to showered  $\mathbb{S}$  events. The remaining positive  $\mathbb{H}$  events are kept unchanged. The showering is performed with PYTHIA8 [9].

For each  $\mathbb{S}$ -event, PYTHIA8 is first run only up to the first QCD shower emission. Since the process considered here has a colour-singlet Born final state, only initial-state QCD radiation can contribute at this stage. We therefore use a PYTHIA8 user hook that vetoes any subsequent shower emission after the first accepted initial-state emission. Hadronisation, multiparton interactions, QED showering and final-state radiation are switched off during this intermediate step. Events with no resolvable emission above the shower cut-off are kept without applying any veto.

<sup>1</sup>In the event generation we set `UseSudakov = .false.` in `madfks_mcatnlo.inc`. This disables the built-in MG5\_AMC option that applies a Sudakov-inspired damping to part of the  $\mathbb{H}$  contribution, so that the input sample corresponds to the standard additive MC@NLO structure of Eqs. (2) and (3).

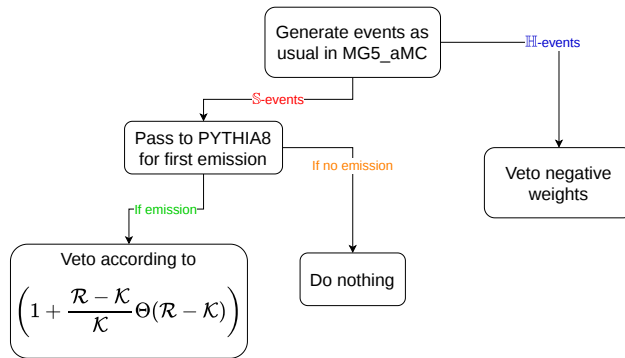


Figure 1: Schematic event-generation workflow used for the MACnLOPS implementation.

For events with one shower emission, the real-emission configuration is used to evaluate the ratio entering Eq. (7). This requires the real matrix element  $\mathcal{R}$  and the Monte Carlo counterterm  $\mathcal{K}$  at the emitted phase-space point. These quantities can be evaluated with existing MG5\_aMC routines, since the same quantities are also needed for the existing MC@NLO matching.

The veto probability is then computed according to Eq. (7), i.e., events in the region  $\mathcal{K} > \mathcal{R}$  are accepted with probability  $\mathcal{R}/\mathcal{K}$ , while events in the region  $\mathcal{R} \geq \mathcal{K}$  are always accepted. The accepted  $\mathbb{S}$  events are then combined with the positive  $\mathbb{H}$  events to form the final MACnLOPS hard-event sample. This sample is passed back to PYTHIA8 for the remaining shower evolution. For accepted  $\mathbb{S}$  events with a first emission, the subsequent shower is started from the scale of that emission.

The full event-generation chain can therefore be summarised as follows:

1. generate an MC@NLO event sample with MG5\_aMC;
2. split the sample into  $\mathbb{S}$  and  $\mathbb{H}$  events;
3. keep the positive  $\mathbb{H}$  events and discard the negative  $\mathbb{H}$  events;
4. shower the  $\mathbb{S}$  events up to the first QCD emission;
5. apply the MACnLOPS veto of Eq. (7) to the emitted  $\mathbb{S}$  events;
6. combine the accepted  $\mathbb{S}$  events with the retained positive  $\mathbb{H}$  events;
7. run the remaining parton shower on the combined event sample.

A schematic overview of the procedure is shown in Fig. 1.

In order to validate the implementation of the MACnLOPS procedure for  $pp \rightarrow ZZ$ , we identify the phase-space regions where the negative  $\mathbb{H}$ -event contributions arise. Figure 2 compares the full input  $\mathbb{H}$ -event contribution (in magenta) with the contribution obtained after retaining only positive  $\mathbb{H}$  events (in green), as a function of the transverse momentum of the final state parton  $p_T^{\text{parton}}$  present in the  $\mathbb{H}$  events before showering. We remind the reader that, due to (transverse) momentum conservation, at this level of predictions we have  $p_T^{\text{parton}} = p_T^{ZZ}$ . In other words, the magenta curves show the  $\mathbb{H}$  events as present in MC@NLO, and in green as present in MACnLOPS. The negative  $\mathbb{H}$  events are concentrated at small  $p_T^{\text{parton}}$ , as expected from the fact that they arise where the shower approximation can locally exceed the real-emission matrix element. They are negligible in the hard tail,

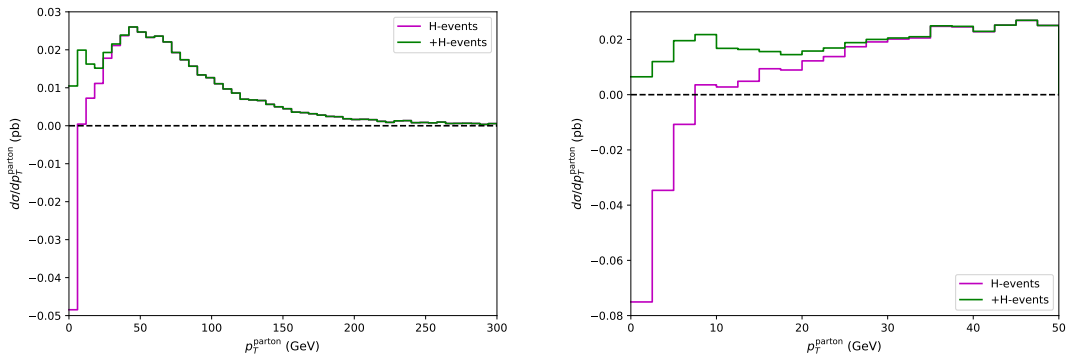


Figure 2: The distributions for the transverse momentum of the final-state parton in the  $\mathbb{H}$  events without discarding the negative ones (magenta), and only positive  $\mathbb{H}$  events (green).

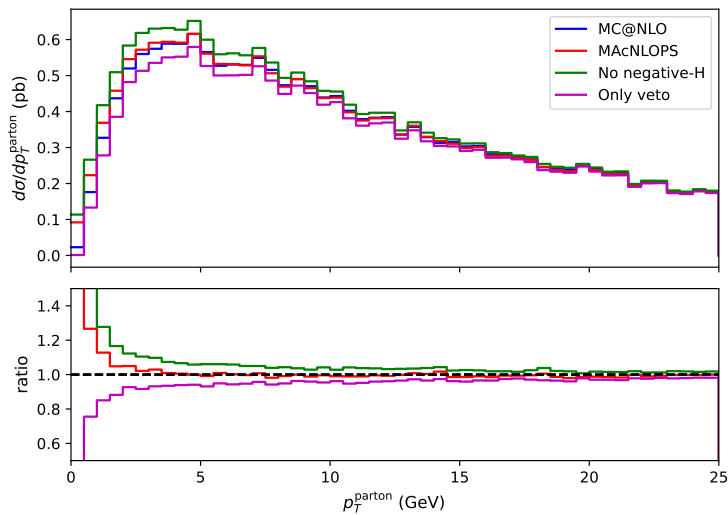


Figure 3: Histograms showing the separate effects of removing negative  $\mathbb{H}$  events and MACnLOPS vetoing, with MACnLOPS and its input MC@NLO for reference.

become visible below roughly  $p_T^{\text{parton}} \simeq 30$  GeV, and dominate the  $\mathbb{H}$  contribution in the lowest bins.

This difference needs to be compensated for by the veto algorithm for the  $\mathbb{S}$  events, after a single emission by the shower. The effect is isolated in Fig. 3 for the low- $p_T^{\text{parton}}$  range. The figure compares the sum of the  $\mathbb{H}$  events and the one-step-showered  $\mathbb{S}$  events. Shown are the distribution for  $p_T^{\text{parton}}$  (i) before removing negative  $\mathbb{H}$  events and vetoing  $\mathbb{S}$  events (this is equal to MC@NLO and labeled as such in the plot); (ii) only removing negative  $\mathbb{H}$  events without applying the veto (in green); (iii) only vetoing the  $\mathbb{S}$  events (in magenta); and (iv) the final MACnLOPS prediction (in red). In the region where  $\mathcal{K} > \mathcal{R}$ , removing the negative  $\mathbb{H}$  term increases the distribution, while the veto on showered  $\mathbb{S}$  events decreases it. Away from the first few bins,  $p_T^{\text{parton}} \gtrsim 2.5$  GeV, these two effects compensate each other at or below the 1% level.

The behaviour in the first bins deserves separate comment. The compensation for the removed negative  $\mathbb{H}$  contribution is not expected to be point-by-point exact. Expanding Eq. (8), the difference between the MACnLOPS and MC@NLO expressions in the region

$\mathcal{K} > \mathcal{R}$  is proportional to

$$\left[ \frac{\tilde{\mathcal{B}}}{\mathcal{B}} \Delta - 1 \right] (\mathcal{R} - \mathcal{K}) \Theta(\mathcal{K} - \mathcal{R}). \quad (10)$$

The replacement  $(\tilde{\mathcal{B}}/\mathcal{B})\Delta \simeq 1$  is sufficient for NLO accuracy because  $\mathcal{R} - \mathcal{K}$  is non-singular, but it need not be numerically a small effect in the immediate vicinity of the shower cut-off. In particular, negative  $\mathbb{H}$  events at an emission scale below the shower cut-off are removed from the sample through the theta function in Eq. (5), but the corresponding  $\mathcal{P}_{\text{veto}}(\Phi)$  for the  $\mathbb{S}$  events is only applied to events that have a shower emission, and are therefore by construction above the shower cut-off. This mismatch is a power-suppressed effect and can formally be neglected; it leads to the MAcNLOPS predictions having a slightly larger rate for  $p_T^{\text{parton}} \gtrsim 2.5$  GeV than the MC@NLO reference.

We can conclude that the MAcNLOPS implementation works as expected for  $pp \rightarrow ZZ$  production. The compensation mechanism for the discarded negative  $\mathbb{H}$  events by the veto on the  $\mathbb{S}$  events is accurate at below the percent level, apart from the power-suppressed region sensitive to the shower cut-off.

## 4 Results

We now compare the MAcNLOPS implementation for  $pp \rightarrow ZZ$  production at the LHC to the default MC@NLO prediction<sup>2</sup>. The event samples contain  $10^5$  hard events at  $\sqrt{s} = 13$  TeV, generated in the five-flavour scheme with fixed renormalisation and factorisation scales  $\mu_R = \mu_F = \sqrt{\hat{s}_B}$ , and parton distribution functions are taken from the CT18NLO set [14]. The subsequent showering is performed with the default  $p_T$ -ordered shower of PYTHIA8 with QED showering, hadronisation and  $Z$  decays switched off. The results are therefore parton-level tests of the matching procedure.

The purpose of the comparison is to show that the MAcNLOPS prediction reproduces the corresponding MC@NLO result within higher-order matching-level effects. Unless explicitly stated otherwise, all figures in this section have a similar layout: a main panel with the reference MC@NLO predictions in blue and the new MAcNLOPS predictions in red, while the lower panel contains the bin-by-bin ratio of MAcNLOPS with MC@NLO. We do not include uncertainty estimates and instead focus on the difference between the central values of the predictions using equivalent input parameters.

The transverse momentum of the  $ZZ$  pair is shown in Fig. 4 (left). The predictions for MAcNLOPS and MC@NLO lie, essentially, on top of each other. The sensitivity to the shower cut-off, as commented on in the discussion below Fig. 3, seems to have disappeared when showering the events. This is not the full story, though. Rather, the MC@NLO prediction shown here, includes the MG5\_AMC option that applies a Sudakov-inspired damping to the low- $p_T$   $\mathbb{H}$  event contribution, see also footnotes 1 and 2. This removes some of the negative  $\mathbb{H}$  events in the low  $p_T$  region, increasing the MC@NLO predictions in the first (couple of) bins, and thereby bringing it closer to MAcNLOPS.

A related radiation-sensitive observable is the azimuthal separation of the two  $Z$  bosons, shown in Fig. 4 (right). At Born level the two bosons are back-to-back, so the limit  $\Delta\phi_{ZZ} \rightarrow \pi$  probes the same recoil region as  $p_T^{ZZ} \rightarrow 0$ . The MAcNLOPS and MC@NLO predictions agree within statistical uncertainties.

<sup>2</sup>Note that, contrary to the previous section, for the MC@NLO predictions, we use the default `UseSudakov = .true.` (see also footnote 1), and therefore these events are no longer identical to the input events to the MAcNLOPS procedure.

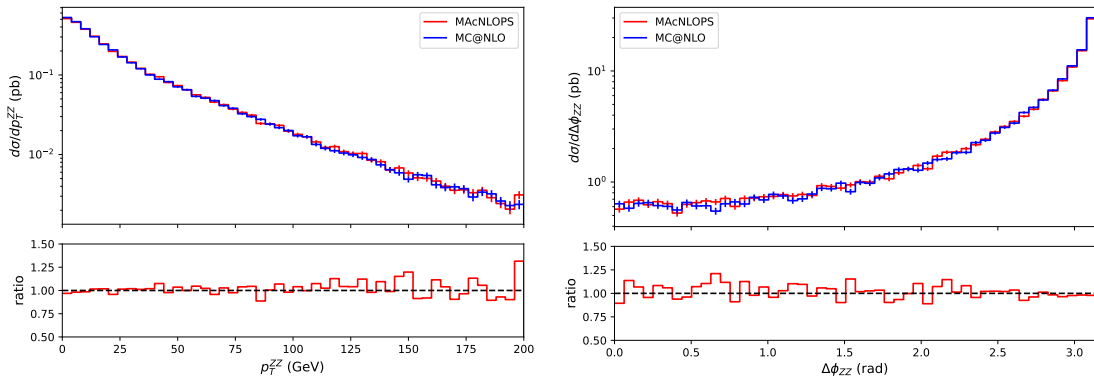


Figure 4: Histograms for the distribution of the transverse momentum of the  $ZZ$  pair (left) and difference in azimuthal angle between the two  $Z$  bosons (right) for MAcNLOPS (in red), with MC@NLO (in blue) as reference, showered with PYTHIA8.

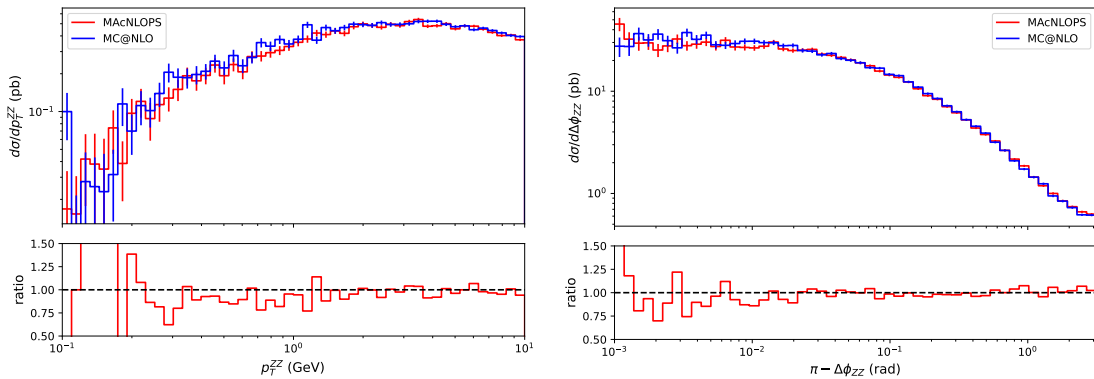


Figure 5: Histograms for  $Z$  boson pair transverse momentum (left) and difference in azimuthal angle of the  $ZZ$ -pair (right) for MAcNLOPS, with MC@NLO and showered with PYTHIA8. Logarithmic binning is employed to emphasize the soft region.

In Fig. 5 we show the  $ZZ$  transverse momentum and the azimuthal separation of the  $ZZ$  system, using logarithmic binning to emphasise the low-scale region. For the azimuthal observable we plot the distribution in  $\pi - \Delta\phi_{ZZ}$ , so that the back-to-back limit is displayed logarithmically. The MAcNLOPS result follows the MC@NLO prediction within statistical uncertainties. A small deficit of MAcNLOPS relative to MC@NLO is visible in the very soft region, related to a power-suppressed dependence on shower cut-off and the Sudakov-inspired damping at low- $p_T$  in the MG5\_AMC implementation of MC@NLO, as explained above.

Finally, the matching procedure should also leave Born-dominated observables unchanged up to higher-order matching effects. Figure 6 shows the invariant mass and rapidity separation of the  $ZZ$  system. These observables are primarily controlled by the underlying Born kinematics and are therefore useful checks that the veto does not bias the hard process. The MAcNLOPS and MC@NLO predictions agree within statistical uncertainties for both observables. This provides a consistency check of the event handling: the additional first-emission processing does not produce a visible distortion of inclusive diboson kinematics.

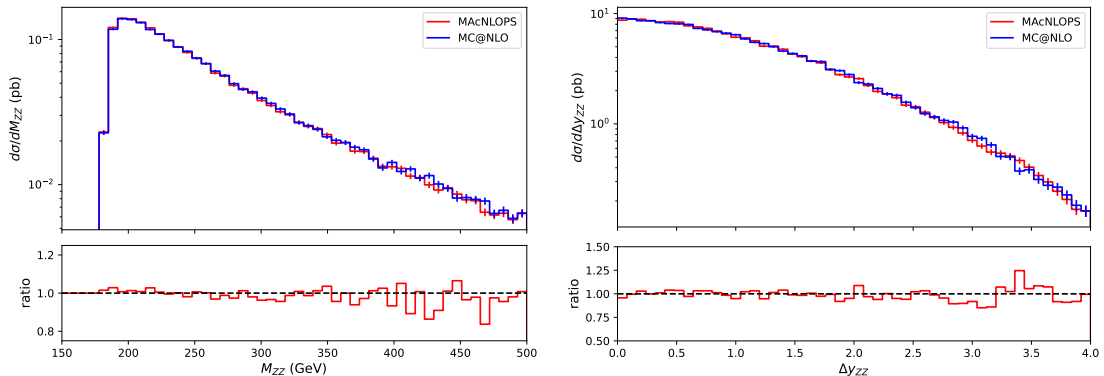


Figure 6: Histograms for invariant mass (left) and rapidity separation (right) of the  $ZZ$ -pair obtained with MACnLOPS (red), with MC@NLO (blue) as reference.

## 5 Conclusions

We have presented a first implementation of the MACnLOPS matching prescription for  $pp \rightarrow ZZ$  production in a MG5\_AMC+PYTHIA8 setup. The implementation follows the minimal construction proposed in Ref. [6]: negative  $\mathbb{H}$  events are removed from the hard-event sample, while their contribution is compensated by applying a veto to the  $\mathbb{S}$  events after the first shower emission. The subsequent shower evolution is then performed with PYTHIA8.

The implementation was validated by comparing MACnLOPS to standard MC@NLO for several observables in  $ZZ$  production. Radiation-sensitive distributions, such as the  $ZZ$  transverse momentum, and the azimuthal separation of the two  $Z$  bosons, show agreement between the present event samples. Inclusive diboson observables, such as the invariant mass and rapidity separation of the two  $Z$  bosons, are also unchanged. These comparisons provide a non-trivial check that the veto procedure compensates the removed negative  $\mathbb{H}$  contribution without producing visible distortions in the matched prediction.

Special attention was paid to the low-scale region, where the cancellation between the removed negative  $\mathbb{H}$  contribution and the vetoed  $\mathbb{S}$  contribution is most delicate. The MACnLOPS result remains compatible with the MC@NLO prediction up to power-suppressed effects. This indicates that the MACnLOPS veto does not introduce an uncontrolled parton-level shape distortion close to the shower cut-off.

The main practical outcome of this study is that the negative  $\mathbb{H}$  weights are removed without introducing a numerically significant extra cost in the event-generation chain. The method does not address negative  $\mathbb{S}$  weights, which can still occur when  $\tilde{\mathcal{B}}(\Phi_B)$  is negative. Combining MACnLOPS with existing methods for reducing negative  $\mathbb{S}$  weights, such as folding [5, 10–12] and/or Born spreading [13], is therefore a natural direction for future work.

The present implementation is tailored to a colour-singlet final state, where the first QCD emission is purely initial-state radiation. It should therefore be directly applicable, or require only minor modifications, for similar colour-singlet production processes with no coloured particles at Born level. Extending the method to processes with final-state radiation or more complicated colour structures will require a more careful treatment of the shower history, the phase-space mapping and the evaluation of the corresponding Monte Carlo counterterms. Such extensions would be important steps towards assessing whether MACnLOPS can provide a general alternative to standard MC@NLO with a substantially

reduced fraction of negative weights.

## References

- [1] S. Frixione and B.R. Webber, *Matching NLO QCD computations and parton shower simulations*, *JHEP* **06** (2002) 029 [[hep-ph/0204244](#)].
- [2] P. Nason, *A New method for combining NLO QCD with shower Monte Carlo algorithms*, *JHEP* **11** (2004) 040 [[hep-ph/0409146](#)].
- [3] S. Frixione, P. Nason and C. Oleari, *Matching NLO QCD computations with Parton Shower simulations: the POWHEG method*, *JHEP* **11** (2007) 070 [[0709.2092](#)].
- [4] S. Jadach, W. Płaczek, S. Sapeta, A. Siódmok and M. Skrzypek, *Matching NLO QCD with parton shower in Monte Carlo scheme — the KrkNLO method*, *JHEP* **10** (2015) 052 [[1503.06849](#)].
- [5] R. Frederix, S. Frixione, S. Prestel and P. Torrielli, *On the reduction of negative weights in MC@NLO-type matching procedures*, *JHEP* **07** (2020) 238 [[2002.12716](#)].
- [6] P. Nason and G.P. Salam, *Multiplicative-accumulative matching of NLO calculations with parton showers*, *JHEP* **01** (2022) 067 [[2111.03553](#)].
- [7] M. van Beekveld, S. Ferrario Ravasio, J. Helliwell, A. Karlberg, G.P. Salam, L. Scyboz et al., *Logarithmically-accurate and positive-definite NLO shower matching*, *JHEP* **10** (2025) 038 [[2504.05377](#)].
- [8] J. Alwall, R. Frederix, S. Frixione, V. Hirschi, F. Maltoni, O. Mattelaer et al., *The automated computation of tree-level and next-to-leading order differential cross sections, and their matching to parton shower simulations*, *JHEP* **07** (2014) 079 [[1405.0301](#)].
- [9] C. Bierlich et al., *A comprehensive guide to the physics and usage of PYTHIA 8.3*, *SciPost Phys. Codeb.* **2022** (2022) 8 [[2203.11601](#)].
- [10] P. Nason, *MINT: A Computer program for adaptive Monte Carlo integration and generation of unweighted distributions*, [0709.2085](#).
- [11] S. Frixione, P. Nason and G. Ridolfi, *The POWHEG-hvq manual version 1.0*, [0707.3081](#).
- [12] S. Alioli, P. Nason, C. Oleari and E. Re, *A general framework for implementing NLO calculations in shower Monte Carlo programs: the POWHEG BOX*, *JHEP* **06** (2010) 043 [[1002.2581](#)].
- [13] R. Frederix and P. Torrielli, *A new way of reducing negative weights in MC@NLO*, *Eur. Phys. J. C* **83** (2023) 1051 [[2310.04160](#)].
- [14] T.-J. Hou et al., *New CTEQ global analysis of quantum chromodynamics with high-precision data from the LHC*, *Phys. Rev. D* **103** (2021) 014013 [[1912.10053](#)].